



Glen R. Gallagher,¹ Michael A. Brehm,² Robert W. Finberg,¹ Bruce A. Barton,³ Leonard D. Shultz,⁴ Dale L. Greiner,² Rita Bortell,² and Jennifer P. Wang¹



Viral Infection of Engrafted Human Islets Leads to Diabetes

Diabetes 2015;64:1358–1369 | DOI: 10.2337/db14-1020

Type 1 diabetes (T1D) is characterized by the destruction of the insulin-producing β -cells of pancreatic islets. Genetic and environmental factors both contribute to T1D development. Viral infection with enteroviruses is a suspected trigger for T1D, but a causal role remains unproven and controversial. Studies in animals are problematic because of species-specific differences in host cell susceptibility and immune responses to candidate viral pathogens such as coxsackievirus B (CVB). In order to resolve the controversial role of viruses in human T1D, we developed a viral infection model in immunodeficient mice bearing human islet grafts. Hyperglycemia was induced in mice by specific ablation of native β -cells. Human islets, which are naturally susceptible to CVB infection, were transplanted to restore normoglycemia. Transplanted mice were infected with CVB4 and monitored for hyperglycemia. Forty-seven percent of CVB4-infected mice developed hyperglycemia. Human islet grafts from infected mice contained viral RNA, expressed viral protein, and had reduced insulin levels compared with grafts from uninfected mice. Human-specific gene expression profiles in grafts from infected mice revealed the induction of multiple interferon-stimulated genes. Thus, human islets can become severely dysfunctional with diminished insulin production after CVB infection of β -cells, resulting in diabetes.

Type 1 diabetes (T1D) is characterized by immune-mediated destruction of the insulin-producing β -cells of the pancreas. Genetic factors, including HLA- and non-HLA-associated loci, contribute to T1D development (1). The association of T1D with interferon (IFN) induced with helicase C domain 1

(*IFIH1*) (2), which senses viral replication intermediates leading to downstream activation of type I IFN, raises viral infection as a possible environmental factor in T1D induction. Compelling evidence supports the etiologic role of enteroviruses in T1D, in particular coxsackievirus B (CVB) (3). A meta-analysis (4) of case-controlled studies revealed a significant association between T1D and enterovirus infection. Enteroviral proteins have been detected in pancreatic tissue specimens from individuals with T1D (5–8). Nevertheless, a definitive link between viral infection and the onset of T1D remains elusive.

Animal models are helpful for understanding virus-induced diabetes but have translational limitations for human disease. For example, coxsackievirus and adenovirus receptor (CAR), the receptor for CVB, is expressed within human islets, but not mouse islets (4,9–11), and infection of C57BL/6 mice with CVB3 or CVB4 does not result in diabetes (unpublished data). NOD mice have been used to extensively assess the parameters of viral infection on T1D, although a critical mass of autoreactive T cells rather than direct viral insult appears to accelerate progression to diabetes during CVB infection (12,13).

Given these inherent limitations, we used the NOD/*Lt-Prkdc^{scid} IL2rg^{tm1WJL}* (NSG) mouse (14) to study the effects of CVB infection in transplanted human islets. NOD mice express multiple alleles that alter the function of the innate and adaptive immune system (15,16). The severe combined immunodeficiency (*scid*) mutation results in a complete absence of T and B lymphocytes. The addition of a targeted null mutation in the interleukin (IL)-2 receptor common γ -chain fully disrupts NK cell development, further reducing innate immune responses, and

¹Department of Medicine, University of Massachusetts Medical School, Worcester, MA

²Program in Molecular Medicine, University of Massachusetts Medical School, Worcester, MA

³Department of Quantitative Health Sciences, University of Massachusetts Medical School, Worcester, MA

⁴The Jackson Laboratory, Bar Harbor, ME

Corresponding author: Jennifer P. Wang, jennifer.wang@umassmed.edu.

Received 3 July 2014 and accepted 4 November 2014.

This article contains Supplementary Data online at <http://diabetes.diabetesjournals.org/lookup/suppl/doi:10.2337/db14-1020/-/DC1>.

The contents of this article are solely the responsibility of the authors and do not necessarily represent the official views of the National Institutes of Health.

© 2015 by the American Diabetes Association. Readers may use this article as long as the work is properly cited, the use is educational and not for profit, and the work is not altered.

facilitating the engraftment of human cells and tissues (17). Hyperglycemia was induced either by administering streptozotocin (STZ) or diphtheria toxin (DT) to NSG mice transgenically expressing the human DT receptor (DTR) under the control of the rat insulin II promoter (the NOD/Lt-Prkdc^{scid} IL2rg^{tm1WJL}Tg(Ins2-HBEGF)6832Ugfm/Sz strain [abbreviated as NSG-Tg(RIP-DTR)]). Hyperglycemic mice were engrafted with human islets to restore normoglycemia and then were infected with CVB4. Our goal was twofold: 1) to assess viral replication and persistence in human islets in vivo and 2) to assess for the development of hyperglycemia. Our results indicate that CVB4 directly invokes the dysfunction of human β -cells, providing insights into the early events that precipitate T1D.

RESEARCH DESIGN AND METHODS

Mice

Mice were maintained in accordance with the Institutional Animal Care and Use Committee of the University of Massachusetts Medical School. NSG male mice, 12–14 weeks old, received a single intraperitoneal injection of 160 mg/kg STZ to induce hyperglycemia (blood glucose >250 mg/dL on 2 consecutive days). B6CBA-Tg(Ins2-HBEGF)6832Ugfm mice, in which the rat insulin II promoter drives β -cell-specific expression of the DTR, were provided by P. Herrera (University of Geneva, Geneva, Switzerland). This transgene was backcrossed using a marker-assisted speed congenic approach to the NSG strain background [i.e., NSG-Tg(RIP-DTR)] (18,19). Female NSG-Tg(RIP-DTR) mice, 12–16 weeks old, were given 40 ng DT by intraperitoneal injection. Nonfasting blood glucose levels were monitored with a glucometer. To enhance survival after the induction of diabetes was confirmed, mice were given LinBit insulin pellet implants (LinShin Canada Inc.) until human islets were available for transplant.

Human Islet Transplantation

Human islets were obtained from the Integrated Islet Distribution Program under protocols approved by the Institutional Review Board of the University of Massachusetts Medical School. A total of 3,000 islet equivalent units were transplanted under the subrenal capsule of each mouse, as previously described (14). For each experiment, islets obtained from single, distinct human donors were used. Mice were allowed to recover from the surgery for 2 weeks to allow for graft revascularization and for normoglycemia to be restored.

Mouse Infections

Mice were intraperitoneally injected with normal saline solution (control) or 1×10^4 plaque-forming units (pfu) of the prototypical CVB4 laboratory strain JVB (catalog # VR-184; American Type Culture Collection) grown in HeLa cells (20). Nonfasting blood glucose levels were measured at least twice weekly. Additional blood samples were obtained weekly for viral RNA extraction. Mice were killed if they displayed gross signs of illness (e.g., ruffling, hunching), and

the native mouse pancreas and the human islet graft were harvested for RNA and histopathology. Serum, pancreas, heart, liver, spleen, and contralateral kidney were harvested for viral titers. Plaque assays were performed using previously described methods (21).

PCR

Viral RNA was extracted from serum using the QIAamp Viral RNA Mini kit (Qiagen) and cDNA generated using the High Capacity cDNA Reverse Transcriptase Kit (Applied Biosystems) followed by quantitative PCR using the Platinum Quantitative PCR SuperMix-UDG Kit (Life Technologies). Enterovirus-specific primers and probe were used for quantification of viral RNA (22). A standard curve was established using the EGFP-CVB3 plasmid as a template (a gift from L. Whitton, Scripps Research Institute, La Jolla, CA) (23).

Histopathology and Immunohistochemistry

Antigen retrieval was performed on paraffin-embedded sections with Retrieval Solution A (BD Biosciences), and endogenous biotin was blocked by Dual Endogenous Enzyme Blocking Reagent (Dako). Guinea pig antibody to insulin (Dako) or rabbit antibody to glucagon (Abcam) was added and detected with the EnVision Dual Link Kit (Dako) followed by staining with DAB Solution (Dako). Samples were counterstained with hematoxylin. A veterinary pathologist scored histopathological changes by blinded scoring of sections.

Immunofluorescence

Antigen retrieval was mediated at 98°C for 45 min in formalin-fixed, paraffin-embedded sections. Sections were blocked with PBS containing 1% BSA and 5% normal goat serum, then incubated with the following primary antibodies overnight: guinea pig antibody to insulin (1:150; Dako); rabbit antibody to glucagon (1:50; Dako); mouse antibody to VP1, clone 5-D8/1 (1:50; Dako); rabbit antibody to cytokeratin 19 (CK19) (1:500; Abcam); and/or rabbit antibody to amylase (1:400; Abcam). Sections were incubated with the following secondary antibodies for 1 h at 1:1,000 dilution: Alexa Fluor-594 goat antibody to guinea pig IgG; Alexa Fluor-647 donkey antibody to rabbit IgG; and Alexa Fluor-488 goat antibody to mouse IgG (catalog #A11076, #A31573, and #A11029, respectively; Life Technologies). Sections were mounted with ProLong Gold Antifade Reagent with DAPI (Life Technologies). Immunofluorescence was imaged on a Leica SP8 confocal microscope and quantified using FIJI software (version 1.48p) using automatic thresholding followed by the measure area function (24). Wide-field images were acquired using a Nikon Eclipse Ni-U microscope with a $\times 4$ plan objective using NIS-Elements imaging software (version 4.13). High-magnification wide-field images were acquired with a $\times 40$ plan objective using QCapture Pro software (version 5.1).

Human Islets for Ex Vivo Studies

Primary human islets from three independent donors were cultured in supplemented CMRL-1066 media and

were challenged with polyinosinic-polycytidylic acid (polyI:C) (InvivoGen) or CVB4. Supernatants were collected at 48 h. TRIzol reagent (Life Technologies) was added for RNA extraction.

Gene Expression Profiling

A multiplex hybridization assay (NanoString) allowed for direct measurement of mRNA copies without the need for amplification. Probes were designed to target human genes in a species-specific manner. The CodeSet included type I IFN, cytokines, apoptosis, endocrine, endoplasmic reticulum (ER) stress, T1D-associated loci, and other human genes, plus seven housekeeping genes for normalization of data. A probe for a conserved CVB sequence targeting the same region as the quantitative RT-PCR primer (20) was included. One hundred nanograms of RNA extracted from tissue was hybridized, processed, and analyzed per the manufacturer's procedure. Data were normalized using the nSolver Analysis Software (version 1.1). Fold changes in gene expression were the ratio of normalized gene expression in CVB4-infected samples versus those in mock-infected samples. Values <1 were transformed by $-1/x$. Averages of fold changes were calculated by averaging the \log_{10} of the fold change followed by a transformation of 10^x . For experiment 2, only five of seven samples from mock-infected mice were analyzed because of space constraints on the NanoString assay.

ELISA

Human IFN- α and IFN- β ELISA kits were from PBL Assay Science. Insulin and C-peptide were quantified using a human-specific ELISA (ALPCO Diagnostics).

Statistical Methods

To compare repeated blood glucose measurements between treatment groups within an experiment, generalized estimating equations were used to adjust for the inherent correlation among the measurements within each mouse. The significance of the regression coefficients was assessed using standard z tests. The relationship between the maximum glucose level and the number of insulin copies and C-peptide level was assessed using Spearman (nonparametric) correlation coefficients with Fisher transformation. The onset of diabetes within and across experiments was compared using Kaplan-Meier product-limit estimates and the log-rank statistic. To assess the significance of the fold-change of gene expression, a standard one-sample t test was used to determine the significance compared with zero. SAS (version 9.3) was used for all analyses.

RESULTS

CVB4-Infected Mice Engrafted With Human Islets Develop Diabetes

β -Cells of the native pancreas were disrupted by treating NSG mice with STZ (experiment 1) or by injecting NSG-Tg (RIP-DTR) mice with DT (experiments 2 and 3). Given the extended kinetics of experiment 1, ablation of native

mouse β -cells was changed to the DTR method, mitigating the possibility of mouse β -cells contributing to glucose homeostasis, which can occur with STZ (25,26). After a hyperglycemic state was confirmed, human donor islets were transplanted into recipient mice to restore normoglycemia. Three independent transplant studies were performed with human islets from donors characterized in Supplementary Table 1. Mice were injected with CVB4 or saline control (mock infected). The target end point of the study was the development of diabetes. At the end of the study, mice were killed, and tissues were harvested for analysis. Supplementary Fig. 1 summarizes survival data for the three studies, and provides the numbers of animals per group plus information on animals that died prematurely and the possible causes of death. Mice that died prematurely were excluded from the final analysis.

In the first experiment, three of six (50%) infected mice that survived >21 days postinfection (dpi) developed diabetes (Fig. 1A, top panel). Mice became hyperglycemic between 21 and 25 dpi, while no mock-infected control mice ($n = 5$) developed diabetes over the course of the experiment (log-rank $P = 0.08$). CVB4 also induced diabetes in experiments 2 and 3, although the kinetics of disease was prolonged. In experiment 2, two of four infected mice (50%) that survived >35 dpi became diabetic (Fig. 1A, middle panel) (log-rank $P = 0.005$). In experiment 3, progression to diabetes was similar to that in experiment 2, with two of five (40%) infected mice surviving >35 dpi becoming diabetic (Fig. 1A, bottom panel) (log-rank $P = 0.09$). Because of the small sample size and the few infected mice that developed diabetes, time to diabetes data were combined across experiments to develop a more stable estimate of the difference between the infected and control mice. Seven CVB4-infected mice developed diabetes with a mean time to diabetes of 28 days, while no control mice developed diabetes (log-rank $P = 0.0002$). The percentage of mice remaining normoglycemic is plotted against time (Fig. 1B).

The peak nonfasting blood glucose value for each mouse over the experimental observation period was assessed and was significantly higher on average for CVB4-infected mice compared with mock-infected mice, which had tightly controlled blood glucose levels throughout (see Supplementary Spreadsheet). Comparing blood glucose levels between CVB4-infected and mock-infected mice with generalized estimating equation models revealed an increase of 81.7 mg/dL in CVB4-infected mice compared with the mock-infected mice ($P = 0.018$) in experiment 1, an increase of 77.5 mg/dL in the infected mice in experiment 2 ($P < 0.0001$) and an increase of 32.0 mg/dL in the infected mice in experiment 3 ($P = 0.07$).

Human insulin and C-peptide levels were compared in terminal serum samples from infected versus control nonfasted mice (Fig. 1C and D). These values were normalized to the terminal serum glucose measurement to account for glycemic variability in nonfasted mice. Lower values were observed in infected mice compared with

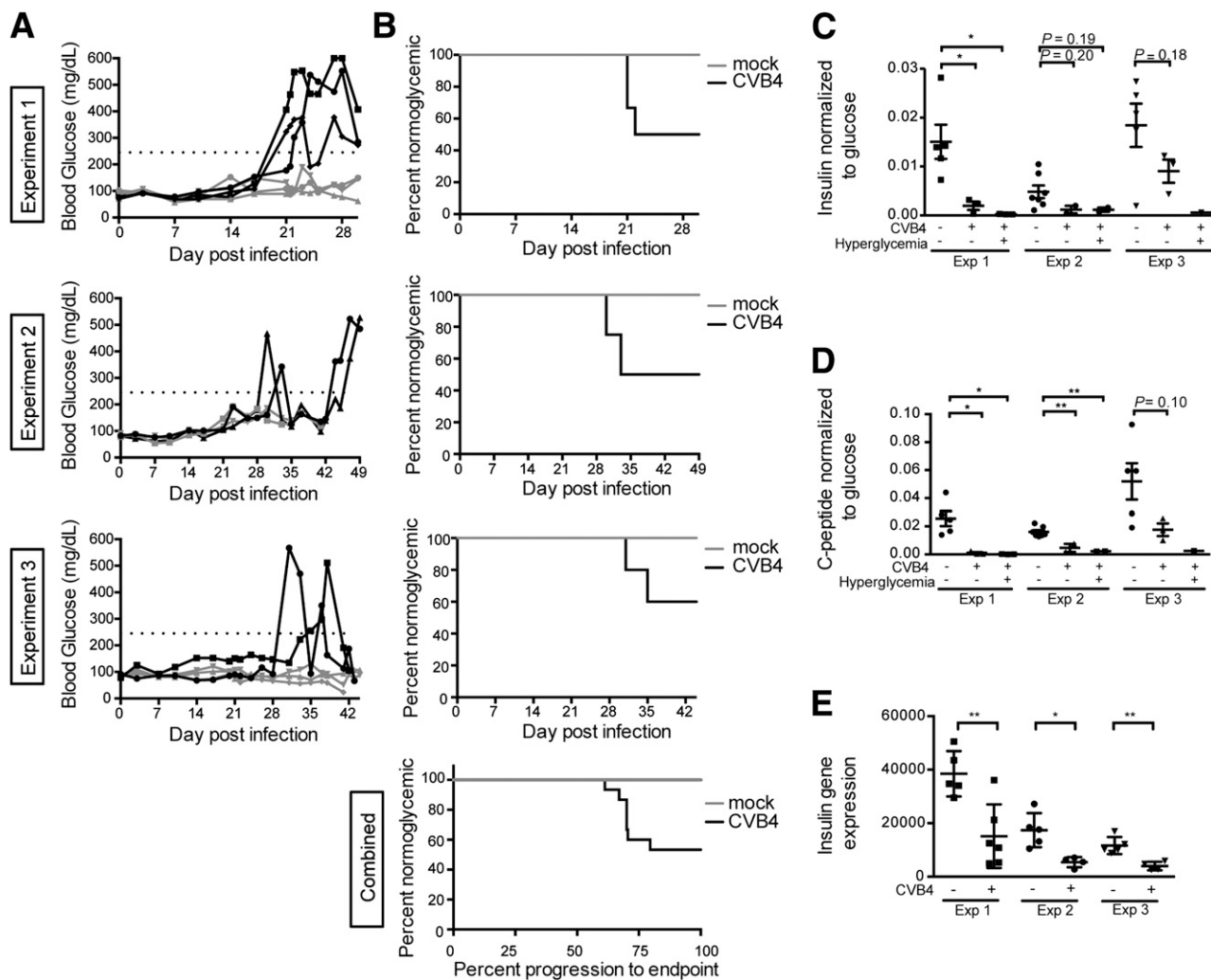


Figure 1—Human islet-engrafted mice exhibit hyperglycemia and low C-peptide and insulin levels after CVB4 infection. **A:** Blood glucose values for nonfasted CVB4-infected animals. Black lines highlight animals that were diabetic. Dotted line indicates 250 mg/dL. **B:** The percentage of animals remaining normoglycemic is shown. Experiment 1, $P = 0.08$; experiment 2, $P = 0.005$; experiment 3, $P = 0.09$, log-rank test. The animals remaining normoglycemic combined from all three experiments is shown (bottom panel) with the time to diabetes onset by the day of diabetes onset by the endpoint for the respective experiment, $P = 0.0002$, log-rank test. Human insulin (**C**) and human C-peptide (**D**) levels as measured by ELISA in terminal serum of nonfasted animals, normalized to the serum glucose level at the time of death. Experiment 1: $n = 5$, mock-infected normoglycemic; $n = 3$, CVB4-infected normoglycemic; $n = 3$, CVB4-infected hyperglycemic. Experiment 2: $n = 7$, mock-infected normoglycemic; $n = 2$, CVB4-infected normoglycemic; $n = 2$, CVB4-infected hyperglycemic. Experiment 3: $n = 5$, mock-infected normoglycemic; $n = 3$, CVB4-infected normoglycemic; $n = 1$, CVB4-infected hyperglycemic. **E:** Human insulin gene expression in grafts measured by NanoString. Values are normalized to a panel of human housekeeping genes. Experiment 1: $n = 5$, mock infected; $n = 6$, CVB4 infected. Experiment 2: $n = 5$, mock infected; $n = 4$, CVB4 infected. Experiment 3: $n = 5$, mock infected; $n = 4$, CVB4 infected. Error bars in **C–E** show the SEM. * $P < 0.05$, ** $P < 0.01$, Student t test. Exp, experiment.

control mice, but no differences were noted between hyperglycemic and normoglycemic infected mice. Insulin (*INS*) gene expression in the human grafts was quantified using NanoString. In each experiment, *INS* gene expression was significantly lower in CVB4-infected mice compared with controls (Fig. 1E). A threefold decrease was observed in *INS* gene expression in grafts from CVB4-infected mice compared with controls (Fig. 5A). In contrast, glucagon (*GCG*) expression ratios were not significantly impacted (Fig. 5B). Thus, regardless of whether overt hyperglycemia was detected, significant decreases in both

human C-peptide and insulin levels were detected in CVB4-infected animals. Across the three experiments, negative correlations were observed between peak blood glucose values and *INS* gene expression (Spearman $\rho = -0.39$, $P = 0.04$). Additionally, negative correlations were observed between peak blood glucose values and terminal serum human C-peptide values ($\rho = -0.45$, $P = 0.01$).

Grafts From Infected Mice Show Decreased Insulin

Histopathological examination of grafts from both CVB4-infected and mock-infected mice revealed intact islets

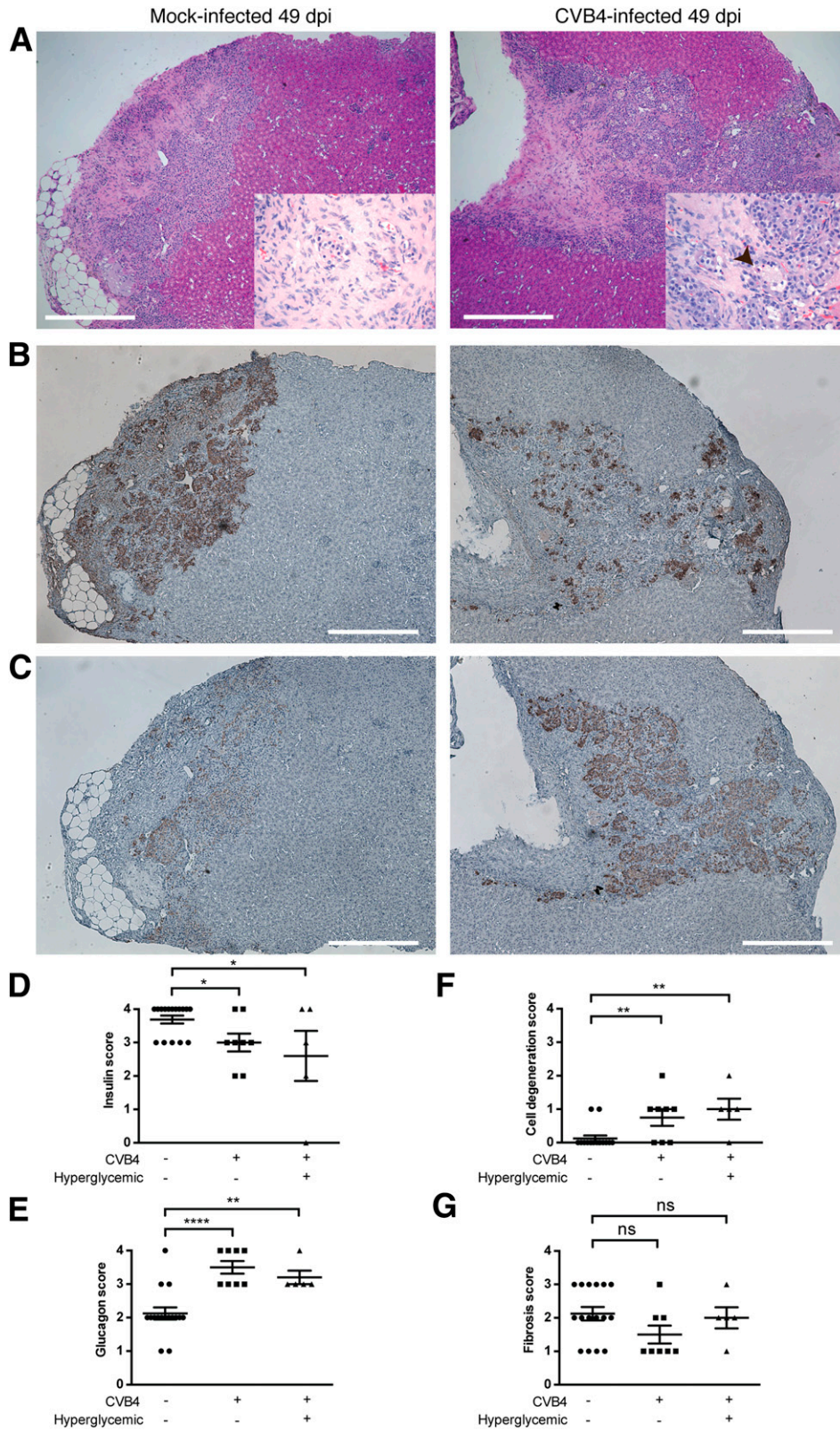


Figure 2—Human islet grafts from CVB4-infected mice have diminished insulin levels compared with grafts from mock-infected control mice. **A:** Hematoxylin-eosin staining on sections of human islet grafts from a representative mock-infected control (left panel) and a CVB4-infected diabetic mouse (right panel) from 49 dpi (experiment 2) shown at $\times 40$ magnification and at $\times 400$ magnification in insets. Scale bars represent 500 μm . In both grafts, islets are surrounded by fibrosis, and surrounding renal cells appear intact. In the CVB4-infected mouse (right panel), degenerative changes are present throughout the engrafted islets. Individual cells are shrunken with karyorrhexis and hyper eosinophilic cytoplasm, and vacuolar degenerative changes are abundant (arrowhead). **B:** Immunohistochemical staining for insulin: $\sim 50\%$ of the graft is positive for insulin in the CVB4-infected mouse (right panel) compared with $>75\%$ in the control mouse (left panel).

without infiltrating inflammatory cells in grafts (Fig. 2A). A moderate degree of fibrosis was present. Insulin-specific immunohistochemical stains revealed a decrease in the number of insulin-positive cells in the islets from infected mice compared with those from control mice (Fig. 2B). Glucagon-specific stains did not reveal glucagon depletion in the grafts of CVB4-infected mice (Fig. 2C). Immunofluorescent staining for insulin and glucagon revealed similar trends (discussed below, see Fig. 3D). Examples are shown from a CVB4-infected mouse that ultimately became diabetic, but the histopathological appearance of grafts from diabetic and nondiabetic CVB4-infected mice were similar overall (see Supplementary Fig. 2). Histopathological changes were quantified by blinded scoring of sections from all available animals (Fig. 2D–G and Supplementary Spreadsheet).

CVB4 Infection Persists in Human Islet-Engrafted Mice

Diabetes did not develop in any infected mice until at least 3 weeks postinfection. Viral RNA was present in mouse serum throughout the course of experiment 1 (Fig. 3A). Plaques were recovered from terminal serum of CVB4-infected animals, indicating the presence of replication-competent virus (Fig. 3B). Viral RNA was readily detected by NanoString from the terminal human graft samples (Fig. 3C). Viral copy numbers were highest in the first experiment, which corresponds with the more rapid time to diabetes compared with the other two experiments. Replicating virus was also present in terminal host tissue samples; examples from experiment 2 include heart ($1.3 \pm 0.6 \times 10^6$ pfu/g, $n = 4$), pancreas ($7.0 \pm 4.0 \times 10^6$ pfu/g, $n = 4$), and the nongrafted kidney ($4.3 \pm 2.1 \times 10^2$ pfu/g, $n = 4$).

To establish that human β -cells were infected with CVB4, coimmunofluorescence staining was performed on human islet graft sections using antibodies against insulin, glucagon, and enterovirus viral protein 1 (VP1). VP1 was readily detected in all graft samples from CVB4-infected mice at various time points; examples from 41 and 49 dpi (Fig. 3D) as well as 7 dpi (Fig. 3E) are shown. Notably, VP1 and insulin colocalized frequently, indicating that β -cells were infected with CVB4. Not all VP1-positive cells were positive for insulin, however, suggesting that other cell populations within human islets can be infected with CVB4. Since exocrine and pancreatic ductal cells can be transplanted along with human islets, we sought to determine whether these cells support viral replication.

Exocrine cells, which stain positive for amylase, were infrequently observed in the grafts, and no evidence of VP1 localization was noted (Fig. 4A). Similarly, CK19-positive pancreatic ductal cells did not colocalize with VP1 (Fig. 4B).

In order to confirm the tropism of CVB for insulin-producing cells in human islets, EGFP-expressing CVB3 was used to infect dispersed cultured human islets *in vitro*. Insulin-positive cells were detected using immunofluorescence staining and visualized by confocal microscopy (Supplementary Fig. 3). EGFP and insulin frequently colocalized, providing further evidence that human β -cells are infected with CVB.

Immunofluorescent staining revealed a significant decrease in the insulin-to-glucagon signal ratio in grafts of infected mice versus control mice. In experiment 2, the insulin-to-glucagon signal ratio was 0.74 ± 0.16 in grafts from CVB4-infected mice ($n = 4$) compared with 3.99 ± 0.92 in mock-infected controls ($n = 6$, $P = 0.02$, Student *t* test). This result was consistent with observations for insulin and glucagon by immunohistochemical staining (Fig. 2).

Gene Expression in Human Islet Grafts Was Profiled

Human graft gene expression levels after infection were assessed using a NanoString platform with species-specific probes. Combined gene expression profile results for 100 genes from graft samples are summarized in Fig. 5A and B. Absolute gene expression values are included in Supplementary Table 2 and Supplementary Spreadsheet. *INS* gene expression was significantly lower in grafts from CVB4-infected mice compared with those from the mock-infected controls (Fig. 1D). Expression values of somatostatin (*SST*) and pancreatic duodenal homeobox-1 (*PDX1*), which regulates transcription of *INS* and *SST*, were also significantly lower in the grafts of CVB4-infected mice relative to those of mock-infected mice.

Numerous genes in the type I IFN pathway, including *CXCL10*, *MX1*, *OAS2*, *CCL5*, *IFIH1*, and *DDX58*, were significantly induced in the grafts of infected mice (Fig. 5B). A moderate but significant increase was observed for *TXNIP*, which encodes thioredoxin-interacting protein and is induced by ER stress through the protein kinase RNA-like ER kinase (PERK) and inositol-requiring enzyme 1 (IRE1) pathways. Expression for *DDIT3*, which encodes CHOP, a multifunctional transcription factor in the ER stress response, was significantly increased. IL-1 β

Scale bars represent 500 μ m. Final magnification is $\times 40$. C: Immunohistochemical staining for glucagon: $\sim 75\%$ of the graft is positive for glucagon in the CVB4-infected mouse (right panel) compared with $\sim 50\%$ in the control mouse (left panel). Scale bars represent 500 μ m. Final magnification is $\times 40$. D: Blinded histopathology scoring of human islet grafts from all available mice: $n = 16$, mock-infected normoglycemic; $n = 8$, CVB4-infected normoglycemic; and $n = 5$, CVB4-infected hyperglycemic. Insulin immunostain, percent positive cells: 0 = 0%, 1 = 25%, 2 = 50%, 3 = 75%, 4 = 90%. E: Glucagon immunostain, percent positive cells: 0 = 0%, 1 = 25%, 2 = 50%, 3 = 75%, 4 = 90%. F: Degeneration of implanted cells: 0 = none, 1 = minimal, 2 = mild, 3 = moderate, 4 = marked. G: Fibrosis of the implanted cells: 0 = none, 1 = minimal, 2 = mild, 3 = moderate, 4 = marked. * $P < 0.05$, ** $P < 0.01$, **** $P < 0.0001$, Student *t* test. A summary table of the blind scoring data is available in the Supplementary Spreadsheet. No differences were observed in scores between infected normoglycemic and hyperglycemic mice.

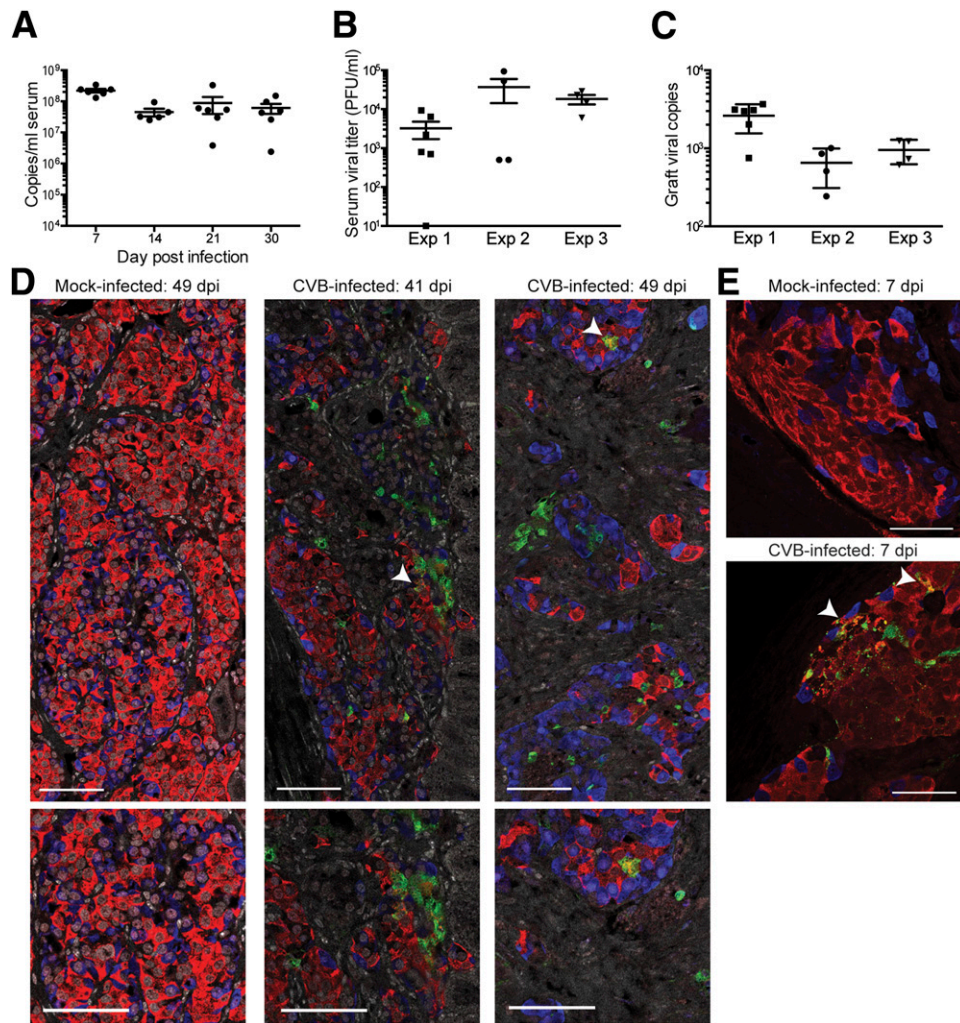


Figure 3—Viral replication is sustained after CVB4 infection of human islet–engrafted mice. **A**: Viral copies, measured by qPCR, are present in serum throughout the duration of the study. Data from experiment 1 are shown. Error bars show the SEM. **B**: Replicating virus is present in serum from CVB4-infected mice at the time of takedown. **C**: Viral nucleic acid, quantified by NanoString, is present in the grafts of CVB4-infected animals at the time of takedown. Experiment 1, $n = 6$. Experiment 2, $n = 4$. Experiment 3, $n = 4$. Grafts from mock-infected animals each had <10 copies by NanoString. **D**: VP1 is present within the grafts of CVB4-infected animals. Arrowheads in top panels show examples of regions positive for both VP1 and insulin and images focused on those areas are shown in bottom panels. Samples from experiment 2 are shown, including those from a mock-infected control (49 dpi) and two CVB4-infected mice (41 and 49 dpi). VP1 is green, glucagon blue, and insulin red. Images were acquired with a $\times 40$ objective. Scale bars represent $75\ \mu\text{m}$. **E**: VP1 is present in insulin-producing cells in grafts of CVB4-infected mice. Samples from an experiment in which grafts were specifically planned for harvest at 7 dpi are shown. VP1 is absent from the graft of a mock-infected control mouse (top panel). VP1 and insulin colocalize in a graft from a CVB4-infected mouse (bottom panel, arrowheads). Scale bars represent $50\ \mu\text{m}$. Acquired with a $\times 63$ objective. Exp, experiment.

gene expression was significantly decreased, although absolute values in samples were consistently low (Supplementary Table 2).

Gene Expression in Cultured Human Islets Was Profiled

Next, cultured islets from three different human donors were independently challenged with CVB4. At 48 h postchallenge, supernatants were harvested and cells were processed for RNA to assess gene expression using the NanoString probes (Fig. 6A and B). Again, significant changes in gene expression were observed

in CVB4-infected samples compared with those from controls. Greatest decreases were again seen with *INS*, *SST*, and *PDX1*, although statistical significance was achieved only with *INS* ($P = 0.034$, 0.071 , and 0.056 , respectively, Student t test). Increases in expression were observed for numerous type I IFN response genes, including *OAS2* and *MX1*, as well as *TLR3* and *IFNB1*. Absolute expression values are included in Supplementary Table 3 and Supplementary Spreadsheet. Low levels of IFN- β and IFN- α were detected in supernatants from cultured human islets 48 h postchallenge with CVB4 or the IFIH1 agonist polyI:C (Fig. 6C).

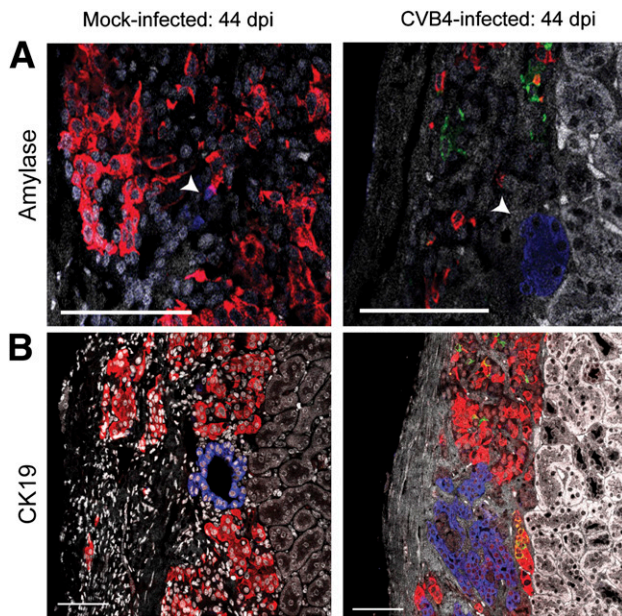


Figure 4—VP1 does not colocalize with human exocrine or ductal cells in the grafts of infected mice. Samples from experiment 3 at 44 dpi are shown for a mock-infected mouse (left panels) or a CVB4-infected mouse (right panels) that did not become diabetic. VP1 is not present in the graft of the mock-infected mouse but is readily detected within the human islet graft of the CVB4-infected mouse (right panels). VP1 (green) associates with insulin (red), but VP1 does not colocalize with amylase (blue)–producing cells (arrowheads) (A) or cells expressing the ductal cell marker CK19 (blue) (B); DAPI is shown in white. Scale bars represent 75 μ m.

DISCUSSION

We describe a model in which NSG mice with induced hyperglycemia are transplanted with human islets and successfully used for studying the viral induction of diabetes. Sustained infection with a prototypical strain of CVB4 is accompanied by reversion to hyperglycemia. Interestingly, the final diabetic state appears to result from a loss of human islet insulin production rather than overt islet destruction. Despite the possibility of resident immune cells being engrafted with the human donor islets, this model provides an environment largely devoid of T cells and antibodies. The absence of an intact immune system in this model provides a new, unobscured view of how viruses can directly initiate diabetes. The diabetic state is most likely a direct consequence of viral infection of human cells that harbor CAR. To our knowledge, this aspect of human specificity has not been previously achieved in other *in vivo* models of viral induction of diabetes. In contrast, other models of virus-induced diabetes depend on the contributions of T cells. For example, β -cell destruction is T cell dependent during the acceleration of diabetes in viral infection of aged NOD mice (27) and in the Kilham rat virus infection model in BBDR rats (28).

Interexperimental variability was observed using several metrics for evaluating diabetes. Fluctuations in blood

glucose measurements for some CVB4-infected mice were noted, but were not entirely unexpected given that glucose levels were randomly obtained from nonfasted animals with concurrent viral disease. Time to the development of diabetes also varied between experiments. The human islets used for engraftment in each experiment were obtained from distinct donors, and differences in the condition of the islets upon transplantation could explain some experimental heterogeneity. Variations in the course of human T1D can be attributed to a multitude of genetic and environmental factors that have only been partially characterized. Despite the different genetic backgrounds of the primary human islets and limited sample sizes, strong patterns in gene expression were noted in islet grafts and in *ex vivo* cultured islets after infection.

Significant changes in gene expression were observed for endocrine genes, type I IFN–associated genes, and T1D susceptibility genes. The endocrine genes *INS*, *SST*, and *PDX1* had the greatest fold decreases in gene expression in both the engrafted islets and *ex vivo*–cultured islets. *PDX1* regulates the expression of both *INS* and *SST*; and protects against apoptosis, autophagy, and susceptibility to ER stress (29–32). Interestingly, persistently infected cultures of a ductal-like cell line with CVB4 have diminished *PDX1* expression after several weeks of infection (33), which provides insights for our model. The expression of type I IFN–associated genes, including *OAS2*, *MX1*, *CCL5*, and *TLR3*, was increased. The presence of a type I IFN signature in individuals genetically at risk for T1D prior to the development of autoantibodies was recently highlighted (34). *CXCL10*, an IFN-stimulated gene, had the highest fold induction of expression in both *in vivo* and *ex vivo* studies. *CXCL10* recruits immune cells at inflammation sites and has been proposed to contribute to the pathogenesis of many autoimmune diseases, including T1D (35,36). T1D susceptibility gene expression for *IFIH1* and *HLA-A* was significantly higher after infection. We previously reported (21) that *IFIH1* mediates IFN responses after CVB infection. Single nucleotide polymorphisms in *IFIH1* that could diminish the type I IFN response after viral infection are associated with protection from T1D (2,37). The marked increase in the expression of *HLA-A* in grafts after infection is consistent with class I MHC hyperexpression described in patients with T1D (38).

The pattern of differentially expressed genes did not completely overlap between the *ex vivo* and *in vivo* studies. The gene expression pattern of cultured human islets 48 h postinfection reflects early responses to viral infection similar to those reported by others (39,40). In contrast, the *in vivo* gene profile in terminal graft samples reflects prolonged consequences of viral infection, and is dominated by downstream cytokines and ER stress-related unfolded protein response genes. Increases in gene expression for *DDIT3*, which encodes CHOP, and *EIF2AK3*, which encodes PERK, were observed; whereas the expression

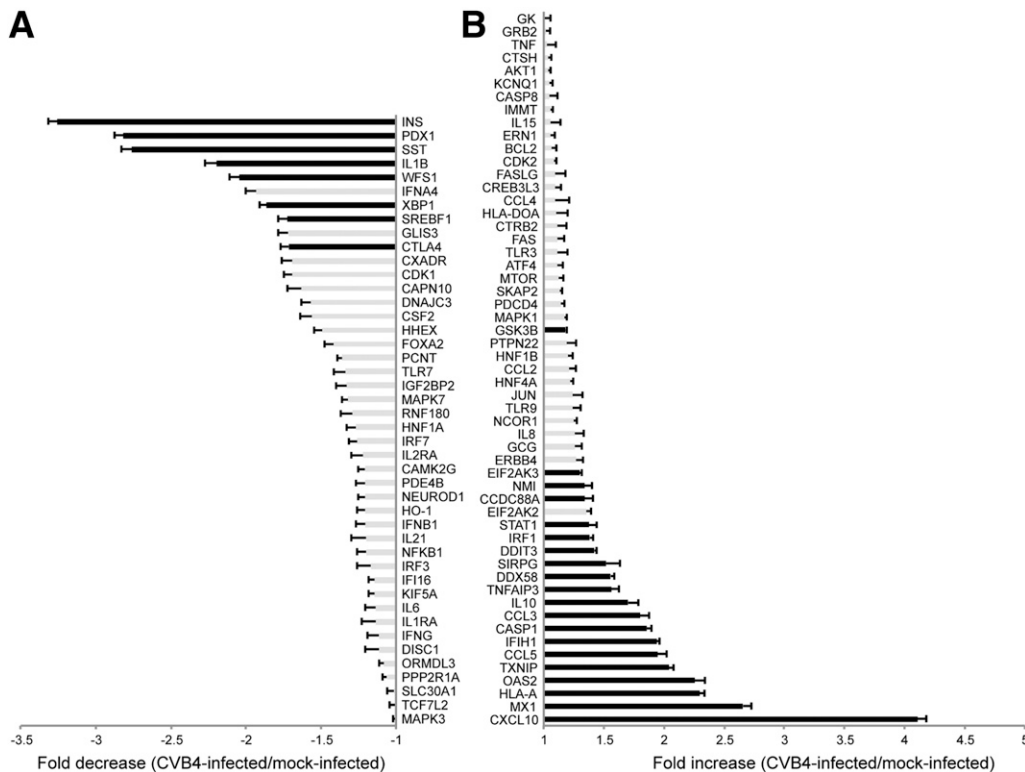


Figure 5—Graft gene expression in CVB4-infected animals by NanoString analysis. *A*: Genes that are decreased in grafts from CVB4-infected mice ($n = 14$) vs. grafts from mock-infected mice ($n = 15$) are shown as a fold decrease. *B*: Genes that are increased in grafts from CVB4-infected mice ($n = 14$) vs. grafts from mock-infected mice ($n = 15$) are shown as a fold increase. Black bars indicate $P < 0.05$, Student t test. Error bars show the SEM. The categorical distributions for the 100 host genes were as follows: type I IFNs, 17; cytokines, 16; T1D, 15; apoptosis, 14; endocrine, 12; ER stress, 9; and other, 17.

of *XBP1* was decreased. Increased CHOP levels, but not *XBP1* protein levels, were reported in islets from tissue sections of T1D patients (41). *TXNIP* was also highly stimulated in grafts from infected mice. In the virus-induced BBDR rat model of diabetes, the IRE1 and PERK ER stress pathways are activated (42); both of these pathways induce *TXNIP* to promote programmed cell death under unresolvable ER stress (43,44).

Human islet–engrafted mice developed diabetes several weeks after infection, during which time replicating virus was readily detected. CVB can cause prolonged infection in immunocompetent mice. Vella and Festenstein (45) reported that CVB4 infection led to persistent infection in the majority of 10 inbred mouse strains. Persistent enteroviral infections have been described in immunodeficient humans, particularly those with agammaglobulinemia (for review, see Galama [46]). Prolonged coxsackievirus antigen shedding was described in a patient with agammaglobulinemia, corresponding to a lack of neutralizing antibody (47). Additionally, B cell–deficient mice infected with CVB3 exhibit persistent viral production up to 45 dpi (48), and CVB3 persistence has been reported in SCID mice (49). Mounting evidence (33,50) exists that coxsackievirus can establish persistent infections in astrocytic cells and ductal cells of the pancreas. In

our study, we performed dual staining for VP1 and CK19 to determine whether ductal cells were acting as a viral reservoir. We did not detect any colocalization, although others have detected viral RNA from primary ductal cells, which is more sensitive than VP1 staining (33). Identification of additional human cells that can be persistently infected could provide insights into relevant viral reservoirs.

The ability to investigate the long-term consequences of viral infection could provide new insights into the homeostatic balance between mechanisms of β -cell function and death. The human islet engraftment model may reflect the earliest stages of the onset of virus-related diabetes prior to the development of autoimmune responses. Many features are reminiscent of cases of fulminant T1D, characterized by rapid onset of hyperglycemia and ketoacidosis resulting from accelerated β -cell failure. Tissue studies reveal the presence of enterovirus in pancreatic islet cells as well as increased expression of innate immune sensors, *CXCL10*, and type I IFN in β -cells and infiltrating immune cells (51,52), underscoring the importance for innate immune signaling pathways. Infection models using humanized mice that include reconstitution of components of the human immune system will yield further insights

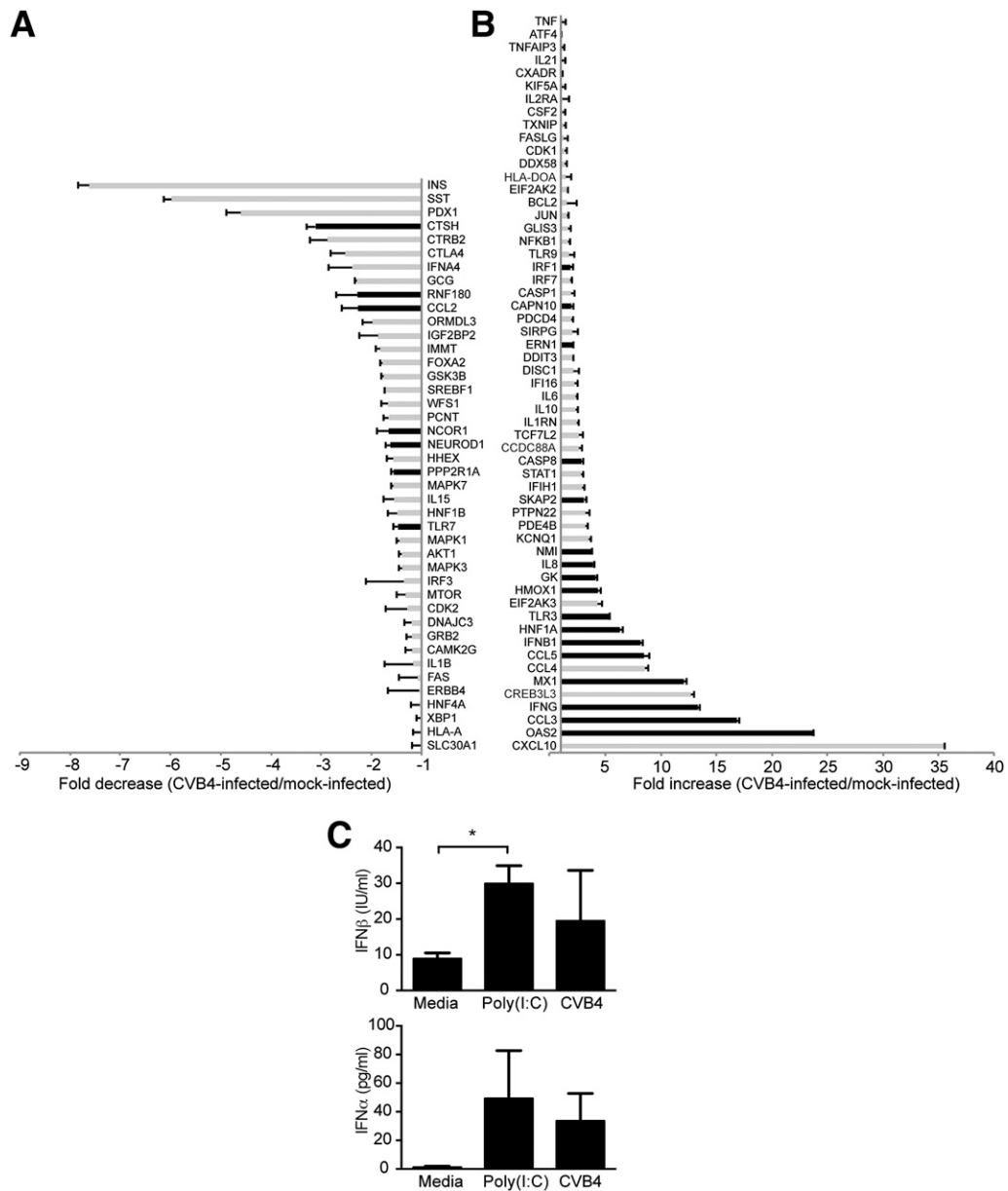


Figure 6—Gene expression in ex vivo-cultured human islets challenged with CVB4. Islets from three independent human donors were challenged with CVB4. At 48 h, supernatants were collected and cells were processed for RNA. **A:** Genes that are decreased in CVB4-infected islets ($n = 3$) vs. mock-infected islets ($n = 3$) are shown as a fold decrease. **B:** Genes that are increased in CVB4-infected islets ($n = 3$) vs. mock-infected islets ($n = 3$) are shown as a fold increase. In **A** and **B**, black bars indicate $P < 0.05$, Student t test. Error bars indicate the SD. **C:** Human IFN- β and IFN- α were measured by ELISA from supernatants of human islets challenged with either CVB4 (10^6 pfu/100 islet equivalent units) or polyI:C (100 μ g/mL) for 48 h. * $P < 0.05$, Student t test. Error bars indicate the SEM.

into the pathogenesis of virus-induced diabetes, revealing specific contributions of both innate and adaptive immunity.

Acknowledgments. The authors thank S. Pham for technical assistance, D. Garlick for histopathology scores, and M. Trombly (University of Massachusetts Medical School) for assistance with manuscript preparation.

Funding. This work was supported in part by National Institutes of Health research grants AI-092105, AI-046629, U01-DK-089572, AI-1112321, and CA-034196 and by Helmsley Charitable Trust grant 2012PG-T1D018.

Duality of Interest. No potential conflicts of interest relevant to this article were reported.

Author Contributions. G.R.G. helped to design the experiments, performed the experiments, and helped to analyze the data and write the manuscript. M.A.B., R.W.F., and D.L.G. helped to design the experiments. B.A.B. performed the statistical analysis. L.D.S. generated the NSG-Tg(RIP-DTR) mice. R.B. helped to design the experiments and analyze the data. J.P.W. helped to design the experiments, analyze the data, and write the manuscript. J.P.W. is the guarantor of this work and, as such, had full access to all the data in the study and takes responsibility for the integrity of the data and the accuracy of the data analysis.

References

1. Concannon P, Rich SS, Nepom GT. Genetics of type 1A diabetes. *N Engl J Med* 2009;360:1646–1654
2. Smyth DJ, Cooper JD, Bailey R, et al. A genome-wide association study of nonsynonymous SNPs identifies a type 1 diabetes locus in the interferon-induced helicase (IFIH1) region. *Nat Genet* 2006;38:617–619
3. Craig ME, Nair S, Stein H, Rawlinson WD. Viruses and type 1 diabetes: a new look at an old story. *Pediatr Diabetes* 2013;14:149–158
4. Yeung WC, Rawlinson WD, Craig ME. Enterovirus infection and type 1 diabetes mellitus: systematic review and meta-analysis of observational molecular studies. *BMJ* 2011;342:d35
5. Dotta F, Censini S, van Halteren AG, et al. Coxsackie B4 virus infection of beta cells and natural killer cell insulinitis in recent-onset type 1 diabetic patients. *Proc Natl Acad Sci U S A* 2007;104:5115–5120
6. Richardson SJ, Willcox A, Bone AJ, Foulis AK, Morgan NG. The prevalence of enteroviral capsid protein vp1 immunostaining in pancreatic islets in human type 1 diabetes. *Diabetologia* 2009;52:1143–1151
7. Richardson SJ, Leete P, Bone AJ, Foulis AK, Morgan NG. Expression of the enteroviral capsid protein VP1 in the islet cells of patients with type 1 diabetes is associated with induction of protein kinase R and downregulation of Mcl-1. *Diabetologia* 2013;56:185–193
8. Willcox A, Richardson SJ, Bone AJ, Foulis AK, Morgan NG. Immunohistochemical analysis of the relationship between islet cell proliferation and the production of the enteroviral capsid protein, VP1, in the islets of patients with recent-onset type 1 diabetes. *Diabetologia* 2011;54:2417–2420
9. Bergelson JM, Cunningham JA, Droguett G, et al. Isolation of a common receptor for Coxsackie B viruses and adenoviruses 2 and 5. *Science* 1997;275:1320–1323
10. Mena I, Fischer C, Gebhard JR, Perry CM, Harkins S, Whitton JL. Coxsackievirus infection of the pancreas: evaluation of receptor expression, pathogenesis, and immunopathology. *Virology* 2000;271:276–288
11. Chehadeh W, Kerr-Conte J, Pattou F, et al. Persistent infection of human pancreatic islets by coxsackievirus B is associated with alpha interferon synthesis in beta cells. *J Virol* 2000;74:10153–10164
12. Tracy S, Drescher KM, Chapman NM, et al. Toward testing the hypothesis that group B coxsackieviruses (CVB) trigger insulin-dependent diabetes: inoculating nonobese diabetic mice with CVB markedly lowers diabetes incidence. *J Virol* 2002;76:12097–12111
13. Pearson T, Markees TG, Wicker LS, et al. NOD congenic mice genetically protected from autoimmune diabetes remain resistant to transplantation tolerance induction. *Diabetes* 2003;52:321–326
14. Jurczyk A, Diiorio P, Brostowin D, et al. Improved function and proliferation of adult human beta cells engrafted in diabetic immunodeficient NOD-scid IL2rgamma(null) mice treated with alogliptin. *Diabetes Metab Syndr Obes* 2013;6:493–499
15. Shultz LD, Schweitzer PA, Christianson SW, et al. Multiple defects in innate and adaptive immunologic function in NOD/LtSz-scid mice. *J Immunol* 1995;154:180–191
16. D'Alise AM, Auyeung V, Feuerer M, et al. The defect in T-cell regulation in NOD mice is an effect on the T-cell effectors. *Proc Natl Acad Sci U S A* 2008;105:19857–19862
17. Shultz LD, Ishikawa F, Greiner DL. Humanized mice in translational biomedical research. *Nat Rev Immunol* 2007;7:118–130
18. Greiner DL, Brehm MA, Hosur V, Harlan DM, Powers AC, Shultz LD. Humanized mice for the study of type 1 and type 2 diabetes. *Ann N Y Acad Sci* 2011;1245:55–58
19. Brehm MA, Powers AC, Shultz LD, Greiner DL. Advancing animal models of human type 1 diabetes by engraftment of functional human tissues in immunodeficient mice. *Cold Spring Harb Perspect Med* 2012;2:a007757
20. Sickles GM, Feorino P, Plager H. Isolation and type determination of Coxsackie virus, group B, in tissue culture. *Proc Soc Exp Biol Med* 1955;88:22–24
21. Wang JP, Cerny A, Asher DR, Kurt-Jones EA, Bronson RT, Finberg RW. MDA5 and MAVS mediate type I interferon responses to coxsackie B virus. *J Virol* 2010;84:254–260
22. Moya-Suri V, Schlosser M, Zimmermann K, Rjasanowski I, Gürtler L, Mentel R. Enterovirus RNA sequences in sera of schoolchildren in the general population and their association with type 1-diabetes-associated autoantibodies. *J Med Microbiol* 2005;54:879–883
23. Feuer R, Mena I, Pagarigan R, Slifka MK, Whitton JL. Cell cycle status affects coxsackievirus replication, persistence, and reactivation in vitro. *J Virol* 2002;76:4430–4440
24. Schindelin J, Arganda-Carreras I, Frise E, et al. Fiji: an open-source platform for biological-image analysis. *Nat Methods* 2012;9:676–682
25. Brehm MA, Bortell R, Diiorio P, et al. Human immune system development and rejection of human islet allografts in spontaneously diabetic NOD-Rag1null IL2rgammanull Ins2Akita mice. *Diabetes* 2010;59:2265–2270
26. Guz Y, Nasir I, Teitelman G. Regeneration of pancreatic beta cells from intra-islet precursor cells in an experimental model of diabetes. *Endocrinology* 2001;142:4956–4968
27. Serreze DV, Ottendorfer EW, Ellis TM, Gauntt CJ, Atkinson MA. Acceleration of type 1 diabetes by a coxsackievirus infection requires a preexisting critical mass of autoreactive T-cells in pancreatic islets. *Diabetes* 2000;49:708–711
28. Guberski DL, Thomas VA, Shek WR, et al. Induction of type I diabetes by Kilham's rat virus in diabetes-resistant BB/Wor rats. *Science* 1991;254:1010–1013
29. Fujimoto K, Hanson PT, Tran H, et al. Autophagy regulates pancreatic beta cell death in response to Pdx1 deficiency and nutrient deprivation. *J Biol Chem* 2009;284:27664–27673
30. Sachdeva MM, Claiborn KC, Khoo C, et al. Pdx1 (MODY4) regulates pancreatic beta cell susceptibility to ER stress. *Proc Natl Acad Sci U S A* 2009;106:19090–19095
31. Johnson JD, Ahmed NT, Luciani DS, et al. Increased islet apoptosis in Pdx1 +/- mice. *J Clin Invest* 2003;111:1147–1160
32. Hayes HL, Moss LG, Schisler JC, et al. Pdx-1 activates islet α - and β -cell proliferation via a mechanism regulated by transient receptor potential cation channels 3 and 6 and extracellular signal-regulated kinases 1 and 2. *Mol Cell Biol* 2013;33:4017–4029
33. Sane F, Caloone D, Gmyr V, et al. Coxsackievirus B4 can infect human pancreas ductal cells and persist in ductal-like cell cultures which results in inhibition of Pdx1 expression and disturbed formation of islet-like cell aggregates. *Cell Mol Life Sci* 2013;70:4169–4180
34. Ferreira RC, Guo H, Coulson RM, et al. A type I interferon transcriptional signature precedes autoimmunity in children genetically at risk for type 1 diabetes. *Diabetes* 2014;63:2538–2550
35. Antonelli A, Ferrari SM, Corrado A, Ferrannini E, Fallahi P. CXCR3, CXCL10 and type 1 diabetes. *Cytokine Growth Factor Rev* 2014;25:57–65
36. Lacotte S, Brun S, Muller S, Dumortier H. CXCR3, inflammation, and autoimmune diseases. *Ann N Y Acad Sci* 2009;1173:310–317
37. Nejentsev S, Walker N, Riches D, Egholm M, Todd JA. Rare variants of IFIH1, a gene implicated in antiviral responses, protect against type 1 diabetes. *Science* 2009;324:387–389
38. Coppieters KT, Dotta F, Amirian N, et al. Demonstration of islet-autoreactive CD8 T cells in insulinitic lesions from recent onset and long-term type 1 diabetes patients. *J Exp Med* 2012;209:51–60
39. Ylipaasto P, Kutlu B, Rasilainen S, et al. Global profiling of coxsackievirus- and cytokine-induced gene expression in human pancreatic islets. *Diabetologia* 2005;48:1510–1522
40. Schulte BM, Lanke KH, Piganelli JD, et al. Cytokine and chemokine production by human pancreatic islets upon enterovirus infection. *Diabetes* 2012;61:2030–2036
41. Marthour I, Lopez XM, Lefkaditis D, et al. Expression of endoplasmic reticulum stress markers in the islets of patients with type 1 diabetes. *Diabetologia* 2012;55:2417–2420

42. Yang C, Diiorio P, Jurczyk A, O'Sullivan-Murphy B, Urano F, Bortell R. Pathological endoplasmic reticulum stress mediated by the IRE1 pathway contributes to pre-insulinitic beta cell apoptosis in a virus-induced rat model of type 1 diabetes. *Diabetologia* 2013;56:2638–2646
43. Osowski CM, Hara T, O'Sullivan-Murphy B, et al. Thioredoxin-interacting protein mediates ER stress-induced β cell death through initiation of the inflammasome. *Cell Metab* 2012;16:265–273
44. Lerner AG, Upton JP, Praveen PV, et al. IRE1 α induces thioredoxin-interacting protein to activate the NLRP3 inflammasome and promote programmed cell death under irremediable ER stress. *Cell Metab* 2012;16:250–264
45. Vella C, Festenstein H. Coxsackievirus B4 infection of the mouse pancreas: the role of natural killer cells in the control of virus replication and resistance to infection. *J Gen Virol* 1992;73:1379–1386
46. Galama JM. Enteroviral infections the immunocompromised host. *Rev Med Microbiol* 1997;8:33–40
47. Johnson JP, Yolken RH, Goodman D, Winkelstein JA, Nagel JE. Prolonged excretion of group A coxsackievirus in an infant with agammaglobulinemia. *J Infect Dis* 1982;146:712
48. Mena I, Perry CM, Harkins S, Rodriguez F, Gebhard J, Whitton JL. The role of B lymphocytes in coxsackievirus B3 infection. *Am J Pathol* 1999;155:1205–1215
49. Chow LH, Beisel KW, McManus BM. Enteroviral infection of mice with severe combined immunodeficiency. Evidence for direct viral pathogenesis of myocardial injury. *Lab Invest* 1992;66:24–31
50. Zhang X, Zheng Z, Shu B, et al. Human astrocytic cells support persistent coxsackievirus B3 infection. *J Virol* 2013;87:12407–12421
51. Aida K, Nishida Y, Tanaka S, et al. RIG-I- and MDA5-initiated innate immunity linked with adaptive immunity accelerates beta-cell death in fulminant type 1 diabetes. *Diabetes* 2011;60:884–889
52. Tanaka S, Nishida Y, Aida K, et al. Enterovirus infection, CXC chemokine ligand 10 (CXCL10), and CXCR3 circuit: a mechanism of accelerated β -cell failure in fulminant type 1 diabetes. *Diabetes* 2009;58:2285–2291